New perspective on spring vegetation phenology and global climate change based on Tibetan Plateau tree-ring data

Bao Yang[a,1], Minhui He[a,b,1], Vladimir Shishov[c,d], Ivan Tychkov[c], Eugene Vaganov[e], Sergio Rossi[f,g], Fredrik Charpentier Ljungqvist[h,i], Achim Bräuning[b], and Jussi Grießinger[b]

[a]Key Laboratory of Desert and Desertification, Northwest Institute of Eco-Environment and Resources, Chinese Academy of Sciences, 730000 Lanzhou, China; [b]Institute of Geography, University of Erlangen-Nürnberg, D-91058 Erlangen, Germany; [c]Mathematical Methods and Information Technology Department, Siberian Federal University, 660075 Krasnoyarsk, Russia; [d]Laboratory of Tree-Ring Structure, V.N. Sukachev Institute of Forest, Siberian Branch of the Russian Academy of Sciences, 660036 Krasnoyarsk, Russia; [e]Siberian Federal University, 660041 Krasnoyarsk, Russia; [f]Département des Sciences Fondamentales, Université du Québec à Chicoutimi, Chicoutimi, G7H2B1 QC, Canada; [9]Key Laboratory of Vegetation Restoration and Management of Degraded Ecosystems, Provincial Key Laboratory of Applied Botany, South China Botanical Garden, Chinese Academy of Sciences, 510650 Guangzhou, China; [h]Department of History, Stockholm University, SE-106 91 Stockholm, Sweden; and [i]Bolin Centre for Climate Research, Stockholm University, SE-106 91 Stockholm, Sweden

Edited by William H. Schlesinger, Cary Institute of Ecosystem Studies, Millbrook, NY, and approved May 22, 2017 (received for review October 7, 2016)

Phenological responses of vegetation to climate, in particular to the ongoing warming trend, have received much attention. However, divergent results from the analyses of remote sensing data have been obtained for the Tibetan Plateau (TP), the world's largest high-elevation region. This study provides a perspective on vegetation phenology shifts during 1960–2014, gained using an innovative approach based on a well-validated, process-based, tree-ring growth model that is independent of temporal changes in technical properties and image quality of remote sensing products. Twenty composite site chronologies were analyzed, comprising about 3,000 trees from forested areas across the TP. We found that the start of the growing season (SOS) has advanced, on average, by 0.28 d/y over the period 1960–2014. The end of the growing season (EOS) has been delayed, by an estimated 0.33 d/y during 1982–2014. No significant changes in SOS or EOS were observed during 1960–1981. April–June and August–September minimum temperatures are the main climatic drivers for SOS and EOS, respectively. An increase of 1 °C in April–June minimum temperature shifted the dates of xylem phenology by 6 to 7 d, lengthening the period of tree-ring formation. This study extends the chronology of TP phenology farther back in time and reconciles the disparate views on SOS derived from remote sensing data. Scaling up this analysis may improve understanding of climate change effects and related phenological and plant productivity on a global scale.

tree rings | cambial activity | plant phenology | climate change | Tibetan Plateau

Phenology has a profound impact on vegetation growth (1), carbon balances of terrestrial ecosystems (2), and climate change feedback mechanisms (3). The importance of phenology has prompted many studies, mainly using ground-based observations (4–7), which provide useful phenological information at the species level. However, such studies are also quite time-intensive and typically focus on a few individuals in restricted geographic areas, which often limits their applicability to larger spatiotemporal scales. Changes in plant phenology can be detected on larger spatial scales through near-surface remote sensing, using digital repeat photography (8), but this approach remains limited to the stand level. Another commonly used approach is satellite remote sensing, which can cover large areas (9–11); however, this method has yielded inconsistent results on the Tibetan Plateau (TP) (9, 12, 13).

The TP, with an average altitude of over 4,000 m above sea level (a.s.l.), covers more than 2 million square kilometers and is strongly affected by ongoing climate change. Due to its vast area, and its position in subtropical latitudes with high incoming solar radiation, changes in vegetation period duration may have major consequences for regional climate and for carbon sequestration in regional ecosystems. Trends of the Normalized Difference Vegetation Index (NDVI) derived from Global Inventory Modeling and Mapping Studies (GIMMS) data, which are obtained from Advanced Very High Resolution Radiometer (AVHRR) data, have indicated that the regionally averaged onset of the spring growth season for alpine steppes and meadows started early from 1982 to the mid-1990s but was delayed from the mid-1990s to 2006 (12). Yu et al. (12) hypothesized that winter and spring warming had resulted in delayed spring growth seasons on the TP. In contrast, Zhang et al. (9) identified a continuous advancing trend in vegetation green-up from 1982 to 2011 on the TP after merging data from the GIMMS NDVI-based start of the vegetation growing season from 1982 to 2000 with Systeme Probatoire d'Observation dela Tarre (SPOT) NDVI-based start of the growing season from 2001 to 2011. Shen et al. (13) argued that the method used by Zhang et al. (9) did not consider the effects of the nongrowing season NDVI on retrieved green-up dates, and spring phenology showed no significant trend during the period 2000–2011 after correcting for the increased nongrowing season NDVI. These claims sparked considerable

Significance

Inconsistent results regarding the rate of change in spring phenology and its relation to climatic drivers on the Tibetan Plateau have been obtained in the past. We introduce and describe here an innovative approach based on tree-ring data, which converts daily weather data into indices of the start (and end) of the growing season. This method provides a unique long-term record of vegetation phenological variability over the period 1960–2014. This approach could further be extended to other forested regions of the world. Scaling up the analysis would provide additional information on phenological responses of terrestrial ecosystems to the ongoing climate change across the Northern Hemisphere.

Author contributions: B.Y. and M.H. designed research; B.Y. and M.H. performed research; V.S., I.T., and E.V. contributed new reagents/analytic tools; B.Y., M.H., V.S., I.T., and E.V. analyzed data; and B.Y., M.H., V.S., E.V., S.R., F.C.L., A.B., and J.G. wrote the paper.

The authors declare no conflict of interest.

This article is a PNAS Direct Submission.

Freely available online through the PNAS open access option.

Data deposition: Tree-ring SOS and EOS data are available from the World Data Center for Paleoclimatology (https://www.ncdc.noaa.gov/paleo/).

[1]To whom correspondence may be addressed. Email: yangbao@lzb.ac.cn or 18794776049@163.com.

This article contains supporting information online at www.pnas.org/lookup/suppl/doi:10.1073/pnas.1616608114/-/DCSupplemental.

controversy regarding the rate and amplitude of change in TP spring phenology, and the extent to which climatic drivers were responsible for any of these purported changes (10, 14–16). It has been suggested that the observed delay in spring growth detected from the mid-1990s to 2006 was a measurement artifact due to the reduced quality of the AVHRR NDVI data since 2001 (9).

These conflicting results can be attributed to inherent defects in satellite remote sensing data quality (9), such as coarse spatiotemporal resolution and limitations in phenology retrieval methodology (13, 17). It is claimed that satellite-derived vegetation indices are easily contaminated by adverse atmospheric conditions, such as varying aerosol concentrations (10, 15). Other background factors, including changes in snow cover (16) or vegetation coverage due to grassland degradation and/or freezing–thawing cycles (10, 14), have been identified as possible causes of inaccuracy, especially in cases in which the signal is weak in vegetation green-up times detected by satellites (13). It is clear that large uncertainties remain in estimates of the remote sensing-derived variability of vegetation phenology and its climate drivers on the TP. Moreover, datasets from satellite remote sensing and ground-based observations only cover the last 30 y, which limits statistical confidence in trend detection. A dataset covering a much longer period would therefore help to resolve current disagreements and increase statistical confidence levels.

Herein, we suggest a method, based on well-validated, process-based, Vaganov–Shashkin (VS)-oscilloscope model simulations of tree-ring growth data (18), to provide a unique record of vegetation phenological variability over the period 1960–2014. In this model (*SI Appendix*, *Materials and Methods*), daily weather station records are used to estimate the daily tree-ring growth rate, which is transformed into a daily rate of xylem cell production. These estimates identify the dates of the first and last differentiated xylem cells, representing the start and the end of the growing season for each year (SOS and EOS, respectively). The simulated integral growth rate during the growing season can be transformed to tree-ring indices by specific procedures used in the model (*SI Appendix*, *Materials and Methods*). Resulting predictions of tree-ring width chronologies can be compared with the actual tree-ring width data. In this study, the model was adjusted until a significant correlation with observations was achieved ($P < 0.05$) (*SI Appendix*, *Materials and Methods* and Fig. S4). Each year of the chronology was thus tied to SOS and EOS values. The method has been validated for conifers using field observations of the relationship between daily temperature and cambial cell division rates (*Materials and Methods*). The objective of this study was (*i*) to provide robust evidence for the variability of phenological records modeled from TP tree-ring data for 1960–2014, and to assess differences between the subperiods 1960–1981 and 1982–2014—the modeled phenological time series are compared with satellite remote sensing-derived phenological data; and (*ii*) to evaluate the relative effects of temperature and precipitation (including snow), with different seasonal targets, on the variability of tree-ring phenology, from the arid to humid TP subregions.

Results

Characteristics of Tree-Ring Phenology over the Period 1960–2014. A clear, advancing trend in SOS was observed across the TP during 1960–2014. The averaged SOS ranged from the middle of May to the middle of June with a site-specific SD (σ) ranging from 8.8 d to 24.9 d (1960–2014) (Fig. 1*A*). The SOS advanced over time at each of the 20 combined sites (*SI Appendix*, Fig. S5). The trend in 60% of the analyzed series was significant at $P \leq 0.01$. In an additional 15% of all series, the trend was significant at $P \leq 0.05$, resulting in a total of 75% of series passing the significance level. However, the advancing trend of SOS was not significant during the period 1960–1981 in any of the four subregions (*SI Appendix*, Table S3), or over the entire study region (Fig. 1*A*). In contrast, during the subperiod 1982–2014, clear ($P < 0.01$) advancing

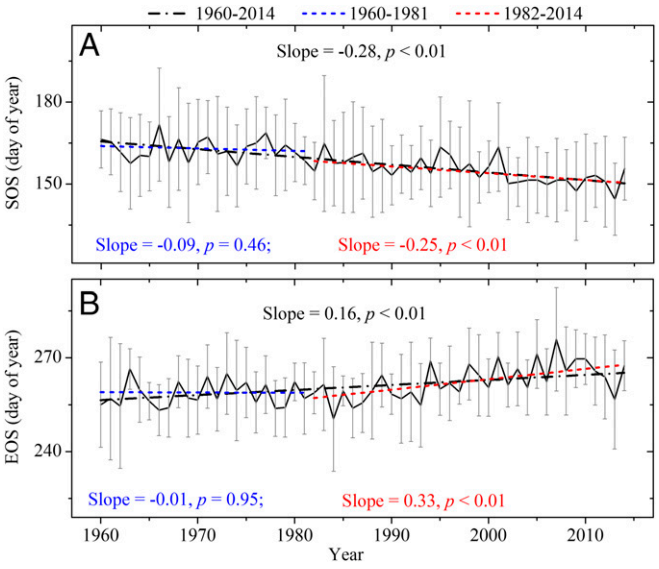

Fig. 1. Characteristics of all of the averaged (*A*) SOS and (*B*) EOS across the study region during the period 1960–2014. Dashed lines indicate linear trends for the periods 1960–2014 (black line), 1982–2014 (red line), and 1960–1981 (blue line). Error bars indicate the SD among the 20 composite sites. Significant ($P < 0.01$) advancing (delaying) trends in SOS (EOS) were detected for the periods 1960–2014 and 1982–2014. During 1960–1981, however, only an insignificant ($P > 0.05$) tendency was identified.

trends were observed in the semihumid and humid subregions (*SI Appendix*, Table S3). Continued but statistically insignificant ($P > 0.01$) SOS advance was seen in each of the four subregions from 2000 to 2014, probably due to the short calibration period (*SI Appendix*, Fig. S6). Over the full study period (1960–2014), significant ($P < 0.01$) advancing trends were observed in all four subregions (*SI Appendix*, Table S3). The rate of advance was −0.28 d/y for the entire study region. From 2000 to 2011, we also found a continued but insignificant advancing trend of all of the averaged SOS (slope = −0.41, $P = 0.17$). However, the advancing trend (slope = −0.80, $P = 0.05$) was significant during 2000–2009. EOS mainly occurred in the middle of September during the period 1960–2014 (Fig. 1*B*). From 1960 to 2014, 80% of the combined sites showed significant ($P < 0.10$) delays (*SI Appendix*, Fig. S7). When the values for all sites were averaged, we noted clear delaying trends for 1960–2014 (0.16 d/y) and 1982–2014 (0.33 d/y) (both $P < 0.01$); whereas the trend for the subperiod 1960–1981 (−0.01 d/y) was not significant ($P = 0.95$) (Fig. 1*B*). Over the period 1960–2014, the length of the growing season (LOS) increased significantly ($P < 0.01$) across all subregions, as well as over the entire TP. From 1982 to 2014, significantly ($P < 0.05$) extended LOSs were identified in all four subregions. On average, the advancing SOS (−0.28 d/y) contributed 64% of the significantly ($P < 0.01$) extended LOSs during the period 1960–2014, whereas 43% of the extension was contributed during the period 1982–2014. In total, due to earlier SOS and delayed EOS, the growing season length increased by 24.2 d during 1960–2014.

Tree-Ring Phenology Response to Climate Variation. The correlation (*SI Appendix*, Fig. S8) between climate factors and SOS from 1960 to 1981 showed that pregrowing season temperatures, especially April through June temperatures, significantly affected SOS at 16 of the tree-ring combined sites ($P < 0.05$; henceforth, all significant correlations refer to $P < 0.05$). Similar temperature factors appeared to drive SOS during 1982–2014 (*SI Appendix*, Fig. S9). Seventeen out of 20 combined sites were significantly influenced by April through June mean, minimum, or maximum temperatures. Such an intensified climatic signal was consistent

with a significant ($P < 0.01$) and recognizable spring warming trend since 1982 (*SI Appendix*, Fig. S10). Over the full study period (1960–2014; *SI Appendix*, Fig. S11), April through June minimum temperatures significantly affected SOS at 18 (90%) of the combined sites. Negative effects of April through June precipitation on SOS were also significant at most of the sampled sites (80% of sites in the arid and semiarid subregions; 60% of sites in the semihumid and humid subregions during the two periods 1982–2014 and 1960–2014) (*SI Appendix*, Figs. S9 and S11). Such correlations indicate that higher preseason precipitation generally results in earlier SOS in the study region. We also checked correlations for SOS and monthly mean and maximum snow depth (*SI Appendix*, Fig. S12). There was no detectable trend or pattern in the snow depth data, suggesting that the influence of snow depth on SOS was, at best, ambiguous. We noted that, on the regional scale, there was a strong correlation with temperature and precipitation from April to June. This correlation was stable during 1982–2014 and throughout the entire study period 1960–2014 (*SI Appendix*, Fig. S13). Partial correlation analyses further revealed that, when controlling for April through June precipitation, the correlation between SOS and April through June minimum temperature was –0.69; when controlling for temperature, the correlation with precipitation was –0.35 during the full period 1960–2014. We thus suggest that the April through June mean minimum temperature has the strongest influence on TP SOS. EOS for all our study subregions was mainly determined by temperatures in the late summer or early autumn (August through September), whereas the effects of precipitation on EOS were statistically insignificant (*SI Appendix*, Figs. S14–16). At most sites, the temperature influence in the subperiod 1960–1981 was lower than that during 1982–2014. However, the September mean, maximum, and minimum temperatures positively ($P < 0.05$) affected TP EOS during all investigated periods (*SI Appendix*, Fig. S17). The highest correlation ($r = 0.78$, $P < 0.01$) was detected between August through September minimum temperatures and EOS during the full 1960–2014 period (Fig. 2). An increase of 1 °C in August through September minimum temperatures resulted in a delay of 6.20 d in EOS.

Discussion

This study developed an innovative approach that combines long-term phenology from remote sensing measurements and tree-ring formation for detecting land surface components in earth system models. Based on the validation of our modeling results with the available monitoring data (*SI Appendix*, *Materials and Methods*), our long-term (1960–2014) tree-ring phenology series is the longest and most robust yet available for the TP.

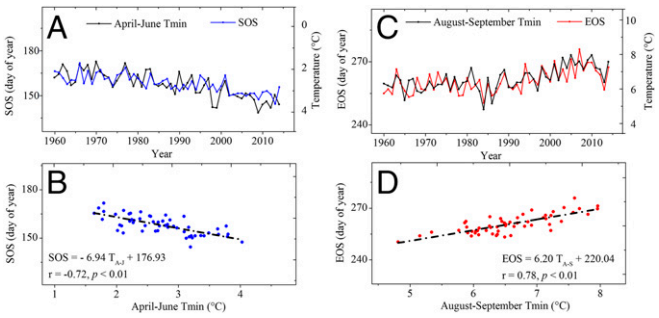

Fig. 2. Comparisons between climate factors and (*A* and *C*) SOS and (*B* and *D*) EOS for the period 1960–2014. Averaged SOS and EOS were mainly driven by April through June minimum temperatures and August through September minimum temperatures, respectively.

Comparison with Remote Sensing Data. According to our modeling results, all averaged tree-ring xylem phenology series showed significant ($P < 0.01$) advancing trends from 1982 to 2014, although different rates were detected within the four subregions of the TP. Contrasting and inconsistent results derived from remote sensing data are mainly explainable by different investigation periods. During the period 1998–2011, a continuous advancing trend (slope = –0.32 d/y, $P = 0.16$) of our averaged SOS was identified. Such an advance was also detected by different remote sensing data from AVHRR, SPOT, and Moderate Resolution Imaging Spectroradiometer (MODIS) (9) over the same period. Moreover, for the different periods of 1998–2014 (slope = –0.24 d/y, $P = 0.18$), 2000–2009 (–0.80 d/y, $P = 0.05$), 2000–2011 (slope = –0.41 d/y, $P = 0.16$), and 2000–2014 (slope = –0.28 d/y, $P = 0.22$), consistent advancing trends of SOS were found by our study. We therefore argue that analysis of a short time series is not sufficient for reliable trend detection, and, instead, a much longer phenological period is critical in resolving current inconsistencies in results derived from remote sensing data. Our approach to establish the longest record of vegetation phenological variability that is also independent of changes in the technical properties of satellite sensors, data coverage, and image quality (e.g., cloudiness) is thus appropriate for addressing such issues.

The methods in determining phenological dates from the remote sensing datasets may also impart some bias. The trend toward earlier vegetation green-up dates (1.9 d per 10 y) detected by the Gaussian-Midpoint and Harmonic Analysis of Time Series (HANTS)-Maximum methods was almost 5 times greater than that detected by the Timesat-Savitzky–Golay (SG) method (0.4 d per 10 y) (19), indicating the uncertainty inherent in such remote sensing methods. The latest vegetation phenological data are based on integrated results by applying multiple methods to remote sensing data (20). The green-up onset dates represent the consolidated annual mean of the plateau-scale green-up date. For the period 2000–2011, the phenological data were derived from four vegetation indices: three NDVIs from AVHRR, SPOT, and MODIS, and one Enhanced Vegetation Index (EVI) from MODIS. For the period 1982–1999, the data were determined from AVHRR NDVI. Five methods were used to derive each vegetation index (for details, see ref. 21). We compared our tree-ring-based phenological series with the remote sensing results of green-up onset dates (20) over the period 1982–2011. They showed similar decreasing trends, confirming that a marked advance of spring phenology has occurred during the past 30 y. Good year-by-year similarity between our modeled SOS and the remote sensing results (20) was also achieved during the common period 1982–2011 (Fig. 3*A*), as indicated by their significant correlation of 0.63 ($P < 0.01$). Moreover, we also found a significant correlation ($r = 0.70$, $P < 0.01$) with the data of regionally averaged green-up dates (9) for meadow and steppe vegetation types throughout the TP during the period 1982–2011 (Fig. 3*A*). It was noted that the remote sensing-retrieved green-up dates were validated by in situ phenological observations from 18 agrometeorological stations on the TP during 2003–2011. However, when comparing our modeled SOS with the AVHRR SOS of meadow vegetation derived using White et al.'s (22) method (12), we found no significant correlation ($r = –0.15$, $P = 0.58$, 1982–1997), probably due to the SOS retrieval method used. We also found significant correlations (Fig. 3*B*) with the end date of the growing season for all vegetation types throughout the TP extracted from AVHRR Leaf Area Index (LAI) data (23) during the period 1982–2011. Moreover, a correlation (Fig. 3*B*) ($r = 0.41$, $P = 0.11$) close to the significant level was found between our modeled EOS and the end date of the growing season for vegetation (meadow) on the TP between 1982–1997 (12), compared with weak negative correlation ($r = –0.15$) between our modeled SOS with the AVHRR

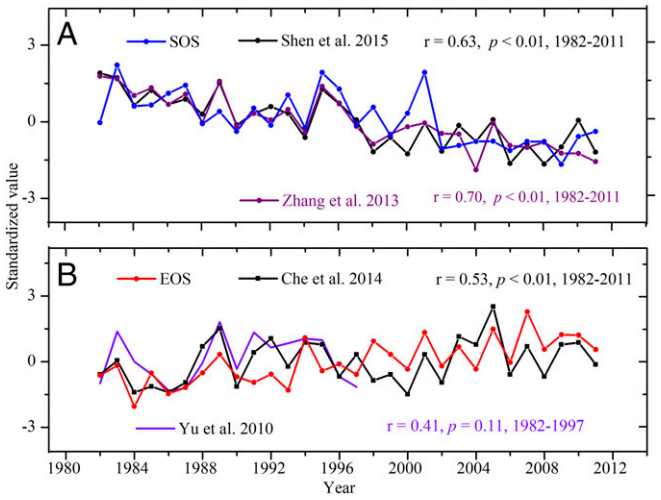

Fig. 3. Comparison of our simulated SOS and EOS with the respective series derived from remote sensing data. (*A*) Shen et al. (20) spring vegetation green-up dates: from 1982 to 1999, as determined from the AVHRR NDVI data using five different methods; and for 2000–2011, extracted with the same five methods from NDVIs observed by AVHRR, MODIS, and SPOT and on the MODIS EVI. The AVHRR sensor was renewed in late 2000 and, because it has been suggested that the AVHRR NDVI data quality has reduced from 2001 onward (9), Zhang et al. (9) spring vegetation green-up dates consist of three time spans: from 1982 to 1997, retrieved from the AVHRR NDVI data; for 1998–1999, retrieved from AVHRR and SPOT NDVI data; and for 2000–2011, retrieved from NDVI datasets observed by MODIS and SPOT. Consistent variability was found between our modeled SOS and remote sensing-based results during 1982–2011. (*B*) Che et al. (23) interannual variations of averaged end dates of vegetation growing season extracted from AVHRR LAI data across the TP during the period 1982–2011 and Yu et al. (12) averaged end dates of meadow vegetation growing season extracted from AVHRR NDVI across the TP. Good agreement is observed among the extracted EOSs. Our results provide an independent reference for comparison.

SOS of vegetation. This finding is understandable because the signal at vegetation green-up times is much weaker and consequently more easily contaminated than at withering times (13, 20).

In summary, our model's predictions and the vegetation green-up series derived from remote sensing data are closely matched for the period 1982–2011. Our model-based tree-ring phenological results reconcile the inconsistency in remote sensing results. We conclude that results combining different vegetation indices and methods may be more accurate than those derived from a single index or method.

It should be noted that tree-ring-based results provide phenological data for the secondary growth of conifers, whereas remote sensing detects the primary growth of vegetation, including the phenology of shrubs and nonwoody species such as grasses or forbs. Conifers are evergreen, and their stem cambium activity may start at any time, as soon as a certain thermal threshold (24) or heat sum (25) is reached. The sensitivity of cambium activity to temperature gradually increases from winter to spring (26), suggesting that either an accumulation of chilling or an increase in day length interact with temperature to initiate the process of cell division in the cambium. However, NDVI data include greening of herbs and grasses during spring resprouting, or annual plants germinating from seed. This process may need a longer time interval or can cause heterogeneities in NDVI response over different vegetation types or regions. Consequently, species-specific or life-form-specific responses of phenology to climate change can be expected. The significant correlation found between remote sensing-derived SOS and our modeling results highlighted that their connection is not casual but robust, although grasses and herbs have more-shallow root systems than trees and therefore might respond differently (27). A 4-y experiment monitoring the growth of spruce and fir on a weekly basis detected synchronism of primary growth (bud and leaf) and secondary (cambium) growth after budburst over the growing season in boreal conifers in eastern Canada (28). Similar synchronism between primary and secondary meristems was identified by direct observations across spruce ecotypes growing in an ordinary garden (29), and this was confirmed on a wider geographical scale by comparing remote sensing chronologies with intraannual data of xylem formation (30). The physiological explanation of the phenological synchronicity between primary and secondary growth remains an issue that is only partially resolved (28).

Overall, this study identified links in the dynamic of meristems across taxa for a longer time interval than previously obtained. Our results provide an independent reference with which to compare results from previous studies based on remote sensing data.

Relationships Between Tree-Ring Phenology and Climate Factors. The April through June minimum temperature appears to have had the highest influence on SOS on the TP during the period 1960–2014, as also demonstrated for other temperate, boreal, and timberline ecosystems in the Northern Hemisphere (24). Because our study region is characterized by high altitudes, it is reasonable that temperature has a significant effect on the starting date of the growing season. As a result, significant correlations between temperature and SOS were obtained by the principle of limiting factor, i.e., that just one factor can have an impact on a biosystem at any particular moment of time in the VS model simulation. Compared with the period 1960–1981, the 1982–2014 phenological data showed a stronger temperature signal, consistent with the observed significant ($P < 0.01$) spring warming after 1982 (*SI Appendix*, Fig. S10). Clearly, increases in April through June minimum temperatures were correlated with the earlier SOS across the whole region (Fig. 2) (see refs. 31–33 for supporting evidence). An increase of 1 °C in April through June minimum temperature caused an advance of 6.94 d in the SOS of our study region (Fig. 2). The results predicted by our model (~7 d per 1 °C) closely matched in situ observations of SOS derived from dendrometer data of Qilian juniper [from an elevational gradient in the northeastern TP (33)] and from microcoring data of European larch from two elevational transects in Switzerland (34). Both studies were based on the so-called "space-for-time/warming experiments" approach (34), whereby long-term changes in the timing and duration of tree growth per shift in degree Celsius (i.e., time) are substituted by changes along altitudinal transects (i.e., space). Monitoring results from 1,321 trees belonging to 10 conifer species located at 39 sites in North America, Europe, and Asia (29.62°N to 66.2°N, 72.87°W to 94.7°E, 60 m a.s.l. to 3,850 m a.s.l.) also revealed that the length of the wood formation period increased linearly at a rate of 6.5 d per 1 °C (24), which is consistent with our results. During winter, the cambium is dormant (35), and growth inactivity of the meristem is maintained even if the environmental requirements (i.e., temperature, water, or day length) are met. In late winter, a change from dormancy to a new state occurs, called quiescence, when growth cannot occur unless the environmentally favorable conditions required are present (26). Favorable thermal conditions speed up cell production rates once dormancy has been broken (36). Warmer spring temperatures also allow cambial cells more time to divide and produce new tracheids. Notably, localized heating experiments have been carried out on tree stems at the end of winter and in early spring, which induced a localized reactivation of the cambium (34, 37). In parts of Europe, a warm spring in 2003 resulted in an earlier onset of cambial activity of around 20 d compared with the succeeding year, 2004 (38). Although these observations were limited to short time periods and small sample sizes, we nonetheless believe that they support our broader argument that spring phenology is mainly driven by temperature variability across large parts of the temperate regions of the Northern Hemisphere.

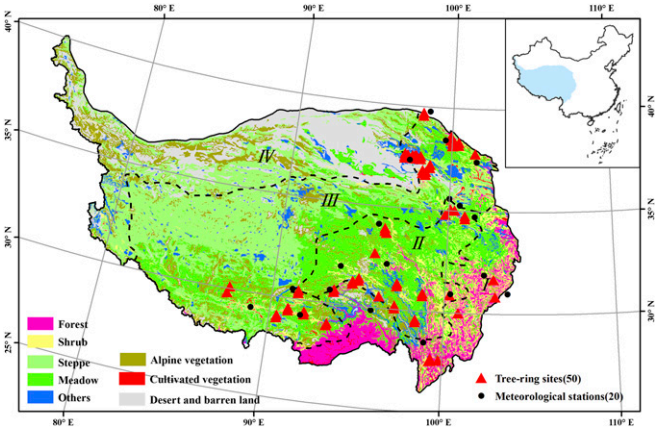

Fig. 4. Map of the study region. Locations of tree-ring sample sites and related meteorological stations on the TP. The black dashed lines indicate the humid (I), semihumid (II), semiarid (III), and arid (IV) subregions. (*Inset*) The location of the study region within China.

Some studies (39–41) emphasized that snow depth and total precipitation also play an important role in regulating spring vegetation phenology. For example, a study based on 3 y of wood anatomical data (2009–2011) from five sampled trees in the arid subregion of the northeastern TP (42) indicated that late spring and early summer precipitation played a critical role in the onset of xylogenesis. If this finding were true, we could expect a strong correlation between SOS and moisture variability in the arid or semiarid subregions, a somewhat weaker correlation in the semihumid or humid subregions and so on, with the limiting role of precipitation decreasing as the subregion becomes more humid. Indeed, we see such a pattern in our results (*SI Appendix*, Fig. S18). We found a stronger influence of May through June precipitation on SOS in the arid and semiarid subregions compared with that in the semihumid and humid subregions during both subperiods 1960–1981 and 1982–2014, as well as in the full study period 1960–2014 (*SI Appendix*, Fig. S18). Remote sensing based results also confirmed that SOS was more sensitive to interannual variations in preseason precipitation in the more arid areas than in the wetter areas of the TP (20).

In conclusion, this study presents an independent series of vegetation phenological records for the TP, covering the period 1960–2014. It is an example of an effective, robust approach to the study of phenological variability in a long-term perspective. The approach, converting daily weather data into the SOS and EOS dates over the growing season based on a well-validated, process-based tree-ring VS model, represents a major advance in the emerging field of phenoclimatology. The generated phenological series serve as a baseline against which to assess previous results based on other methods. Regular studies using this approach should be conducted to cross-validate observational, remote sensing, and in situ (phenocam) estimates of climate-driven trends in phenological patterns. Scaling up this analysis would provide additional information on phenological responses of terrestrial ecosystems to ongoing climate change across the Northern Hemisphere.

Materials and Methods

Study Area. The study area covers the TP, which extends from 27°N to 40°N and from 90°E to 101°E, with an average altitude of more than 4,000 m a.s.l. The dominant vegetation types from southeast to northwest include forest (broadleaf forest, coniferous and broadleaf mixed forest, and coniferous forest), shrub, alpine meadow, alpine steppe, and desert, as well as some intrazonal vegetation types, such as alpine vegetation and cultivated vegetation (Fig. 4). Scattered tree stands (mostly of juniper trees, *Juniperus tibetica*) occur as relict forests, growing mainly on south-facing slopes up to 4,700 m a.s.l (43). To facilitate comparisons, we sorted the locations of all available single-site records into one of four defined climatic subregions (44) (Fig. 4 and *SI Appendix*, Tables S1 and S2).

Chronology Construction. We used 50 single-site tree-ring width series covering the period 1960–2014, in whole or in part. Forty-one series comprised raw measurement data; the others were published standardized tree-ring width chronologies: one from Yikeshu (45) and eight from sites at Zhongtie, Jiangqun, Ningmute, Gongjue, Basu, Mangkang, Bianbamx, and Luolong taken from ref. 46. In total, data from 3,006 trees were used in this study. We grouped them into 20 composite sites based on the concordance between chronologies (*SI Appendix*, Table S2). Matches were required to be significantly correlated at $P < 0.01$. The mean tree-ring series intercorrelation, signal-to-noise ratio, and expressed population signal of the composite chronologies listed in *SI Appendix*, Table S2 further justified combining the single-site series.

Raw measurement data were processed following standard dendrochronological practice (47, 48). The standardized chronologies were used for successive analyses. No significant differences were found when detrending was carried out using a smoothing spline or a negative exponential function.

Tree-Ring Growth Process Modeling. We used an updated tree-ring physiological VS procedure (VS-oscilloscope, vs-genn.ru/downloads/) to model the tree-ring growth process and associated climatic drivers (18). The simulation can be improved by a priori adjustments of its parameters to reflect local tree growth conditions more accurately (18, 49). The daily time resolution is one of the strengths of the process model; it is therefore superior to satellite remote sensing data, which have a resolution that can range between 10 d and half a month. The process model is thus capable of accurately simulating the response of tree-ring growth to rapidly changing climatic variations (18, 49). For details and validation of the models, see *SI Appendix*.

Statistical Analyses. Trends in tree-ring phenological series were calculated using linear least-squares regression; the statistical significance levels were estimated with two-tailed significance tests. Correlations with climate data were analyzed using the software DendroClim2002 (50) during their common periods. Twenty adjoining climate stations close to the tree-ring sampling sites were selected for analysis, starting with the earliest in 1955 and all ending in 2014. We also obtained data for monthly mean and monthly maximum snow depth (51) to explore their relationship with tree-ring phenology variability for the years 1979–2014, i.e., the period for which comparable datasets were available. Partial correlation analyses were performed to determine the most important factors influencing tree-ring phenological variability.

ACKNOWLEDGMENTS. We are grateful to the three anonymous reviewers for their invaluable comments. We are grateful to Q. B. Zhang, Z. S. Li, and X. H. Gou for providing the tree-ring data; to T. Che, L. Y. Dai, and L. Xiao for forwarding the snow depth dataset; to J. C. Xu and H. Y. Yu for providing phenological data; to C. Qin, M. Song, X. Wang, and T. Yang for doing support in simulation; to Prof. Quansheng Ge, Prof. Kathleen A. Campbell, David Chandler, and Martin Cregeen for suggestions and language edits; and to the National Natural Reserve of the Qilian Mountains for logistic support. We acknowledge the International Tree-Ring Data Bank as the source of some of our tree-ring data. This study was jointly funded by the National Natural Science Foundation of China (Grants 41520104005, 41325008, and 41661144008). V.S. and I.T. were supported by the Russian Science Foundation (Grant 14-14-00219P). V.S. acknowledges the support of the Chinese Academy of Sciences President's International Fellowship for Visiting Scientists (Grant 2016VEC033). M.H. appreciates the support of the Alexander von Humboldt Foundation.

1. Myneni RB, Keeling CD, Tucker CJ, Asrar G, Nemani RR (1997) Increased plant growth in the northern high latitudes from 1981 to 1991. *Nature* 386:698–702.
2. Piao S, Friedlingstein P, Ciais P, Viovy N, Demarty J (2007) Growing season extension and its impact on terrestrial carbon cycle in the Northern Hemisphere over the past 2 decades. *Glob Biogeochem Cycles* 21:GB3018.
3. Bonan GB (2008) Forests and climate change: Forcings, feedbacks, and the climate benefits of forests. *Science* 320:1444–1449.
4. Ge QS, Wang H, Rutishauser T, Dai J (2015) Phenological response to climate change in China: A meta-analysis. *Glob Change Biol* 21:265–274.
5. Fu YH, et al. (2015) Declining global warming effects on the phenology of spring leaf unfolding. *Nature* 526:104–107.
6. Menzel A, Fabian P (1999) Growing season extended in Europe. *Nature* 397:659.
7. Chen X, An S, Inouye DW, Schwartz MD (2015) Temperature and snowfall trigger alpine vegetation green-up on the world's roof. *Glob Change Biol* 21:3635–3646.

8. Richardson AD, Klosterman S, Toomey M (2013) Near-surface sensor derived phenology. *Phenology: An Integrative Environmental Science*, ed Schwartz MD (Kluwer Academic, Dordrecht, The Netherlands).
9. Zhang G, Zhang Y, Dong J, Xiao X (2013) Green-up dates in the Tibetan Plateau have continuously advanced from 1982 to 2011. *Proc Natl Acad Sci USA* 110:4309–4314.
10. Luedeling E, Yu H, Xu J (2011) Replies to Shen, Chen et al., and Yi and Zhou: Linear regression analysis misses effects of winter temperature on Tibetan vegetation. *Proc Natl Acad Sci USA* 108:E95.
11. Garonna I, et al. (2014) Strong contribution of autumn phenology to changes in satellite-derived growing season length estimates across Europe (1982-2011). *Glob Change Biol* 20:3457–3470.
12. Yu H, Luedeling E, Xu J (2010) Winter and spring warming result in delayed spring phenology on the Tibetan Plateau. *Proc Natl Acad Sci USA* 107:22151–22156.
13. Shen M, et al. (2013) No evidence of continuously advanced green-up dates in the Tibetan Plateau over the last decade. *Proc Natl Acad Sci USA* 110:E2329.
14. Chen H, Zhu Q, Wu N, Wang Y, Peng CH (2011) Delayed spring phenology on the Tibetan Plateau may also be attributable to other factors than winter and spring warming. *Proc Natl Acad Sci USA* 108:E93.
15. Yi S, Zhou Z (2011) Increasing contamination might have delayed spring phenology on the Tibetan Plateau. *Proc Natl Acad Sci USA* 108:E94.
16. Dong J, Zhang G, Zhang Y, Xiao X (2013) Reply to Wang et al.: Snow cover and air temperature affect the rate of changes in spring phenology in the Tibetan Plateau. *Proc Natl Acad Sci USA* 110:E2856–E2857.
17. Ding M, et al. (2015) Start of vegetation growing season on the Tibetan Plateau inferred from multiple methods based on GIMMS and SPOT NDVI data. *J Geogr Sci* 25: 131–148.
18. Shishov VV, et al. (2016) VS-oscilloscope: A new tool to parameterize tree radial growth based on climate conditions. *Dendrochronologia* 39:42–50.
19. Cong N, et al. (2013) Changes in satellite-derived spring vegetation green-up date and its linkage to climate in China from 1982 to 2010: A multimethod analysis. *Glob Change Biol* 19:881–891.
20. Shen M, et al. (2015) Plant phenological responses to climate change on the Tibetan Plateau: Research status and challenges. *Natl Sci Rev* 2:1–14.
21. Shen M, et al. (2014) Increasing altitudinal gradient of spring vegetation phenology during the last decade on the Qinghai–Tibetan Plateau. *Agric For Meteorol* 189-190: 71–80.
22. White MA, Thornton PE, Running SW (1997) A continental phenology model for monitoring vegetation responses to interannual climatic variability. *Glob Biogeochem Cycles* 11:217–234.
23. Che M, et al. (2014) Spatial and temporal variations in the end date of the vegetation growing season throughout the Qinghai–Tibetan Plateau from 1982 to 2011. *Agric For Meteorol* 189-190:81–90.
24. Rossi S, et al. (2016) Pattern of xylem phenology in conifers of cold ecosystems at the Northern Hemisphere. *Glob Change Biol* 22:3804–3813.
25. Seo JW, Eckstein D, Jalkanen R, Rickebusch S, Schmitt U (2008) Estimating the onset of cambial activity in Scots pine in northern Finland by means of the heat-sum approach. *Tree Physiol* 28:105–112.
26. Oribe Y, Kubo T (1997) Effect of heat on cambial reactivation during winter dormancy in evergreen and deciduous conifers. *Tree Physiol* 17:81–87.
27. Eggemeyer KD, et al. (2009) Seasonal changes in depth of water uptake for encroaching trees *Juniperus virginiana* and *Pinus ponderosa* and two dominant C_4 grasses in a semiarid grassland. *Tree Physiol* 29:157–169.
28. Huang JG, Deslauriers A, Rossi S (2014) Xylem formation can be modeled statistically as a function of primary growth and cambium activity. *New Phytol* 203:831–841.
29. Perrin M, Rossi S, Isabel N (2017) Synchronisms between bud and cambium phenology in black spruce: Early-flushing provenances exhibit early xylem formation. *Tree Physiol* 37:593–603.
30. Antonucci S, et al. (2017) Large-scale estimation of xylem phenology in black spruce throughremote sensing. *Agric For Meteorol* 233:92–100.
31. Rossi S, et al. (2008) Critical temperatures for xylogenesis in conifers of cold climates. *Glob Ecol Biogeogr* 17:696–707.
32. Rossi S, Deslauriers A, Anfodillo T, Carraro V (2007) Evidence of threshold temperatures for xylogenesis in conifers at high altitudes. *Oecologia* 152:1–12.
33. Wang Z, Yang B, Deslauriers A, Bräuning A (2014) Intra-annual stem radial increment response of Qilian juniper to temperature and precipitation along an altitudinal gradient in northwestern China. *Trees (Berl)* 29:25–34.
34. Moser L, et al. (2010) Timing and duration of European larch growing season along altitudinal gradients in the Swiss Alps. *Tree Physiol* 30:225–233.
35. Begum S, Nakaba S, Oribe Y, Kubo T, Funada R (2007) Induction of cambial reactivation by localized heating in a deciduous hardwood hybrid poplar (*Populus sieboldii* x *P. grandidentata*). *Ann Bot (Lond)* 100:439–447.
36. Rossi S, et al. (2013) A meta-analysis of cambium phenology and growth: Linear and non-linear patterns in conifers of the northern hemisphere. *Ann Bot (Lond)* 112: 1911–1920.
37. Gričar J, Zupančič M, Čufar K, Oven P (2007) Regular cambial activity and xylem and phloem formation in locally heated and cooled stem portions of Norway spruce. *Wood Sci Technol* 41:463–475.
38. Deslauriers A, Rossi S, Anfodillo T, Saracino A (2008) Cambial phenology, wood formation and temperature thresholds in two contrasting years at high altitude in southern Italy. *Tree Physiol* 28:863–871.
39. Wu X, Liu H (2013) Consistent shifts in spring vegetation green-up date across temperate biomes in China, 1982–2006. *Glob Change Biol* 19:870–880.
40. Wang T, Peng S, Lin X, Chang J (2013) Declining snow cover may affect spring phenological trend on the Tibetan Plateau. *Proc Natl Acad Sci USA* 110:E2854–E2855.
41. Shen M, Piao S, Cong N, Zhang G, Jassens IA (2015) Precipitation impacts on vegetation spring phenology on the Tibetan Plateau. *Glob Change Biol* 21:3647–3656.
42. Ren P, Rossi S, Gricar J, Liang E, Cufar K (2015) Is precipitation a trigger for the onset of xylogenesis in *Juniperus przewalskii* on the north-eastern Tibetan Plateau? *Ann Bot (Lond)* 115:629–639.
43. Miehe G, et al. (2009) How old is pastoralism in Tibet? An ecological approach to the making of a Tibetan Landscape. *Palaeogeogr Palaeoclimatol Palaeoecol* 276:130–147.
44. Zheng JY, et al. (2013) [The climate regionalization in China for 1981–2010]. *Chin Sci Bull* 58:3088–3099. Chinese, with English abstract.
45. Zhang J, et al. (2015) Forward modeling analyses of Qilian Juniper (*Sabina przewalskii*) growth in response to climate factors in different regions of the Qilian Mountains, northwestern China. *Trees (Berl)* 30:175–188.
46. Zhang QB, Evans MN, Lyu L (2015) Moisture dipole over the Tibetan Plateau during the past five and a half centuries. *Nat Commun* 6:8062.
47. Holmes RL (1983) Computer-assisted quality control in tree-ring dating and measurement. *Tree-Ring Bull* 43:69–78.
48. Cook ER, Peters K (1997) Calculating unbiased tree-ring indices for the study of climatic and environmental change. *Holocene* 7:361–370.
49. He MH, et al. (2017) Process-based modeling of tree-ring formation and its relationships with climate on the Tibetan Plateau. *Dendrochronologia* 42:31–41.
50. Biondi F, Waikul K (2004) DENDROCLIM2002: A C++ program for statistical calibration of climate signals in tree-ring chronologies. *Comput Geosci* 30:303–311.
51. Che T, Li X, Jin R, Armstrong R, Zhang TJ (2008) Snow depth derived from passive microwave remote-sensing data in China. *Ann Glaciol* 49:145–154.